RSC Advances

ROYAL SOCIETY OF CHEMISTRY

www.rsc.org/advances

ARTICLE TYPE www. rsc.org/xxxxxx | XXXXXXXX

Unveiled magnetic transition in Na battery material: μ^+SR study of P2-$Na_{0.5}VO_2$

Jun Sugiyama,*[a,b] Izumi Umegaki,[a] Daniel Andreica,[c] Christopher Baines,[d] Alex Amato,[d] Marie Guignard,[e] Claude Delmas,[e] and Martin Månsson[f]

Received Xth XXXXXXXXXX 20XX, Accepted Xth XXXXXXXXX 20XX
First published on the web Xth XXXXXXXXXX 200X
DOI: 10.1039/b000000x

We have investigated the microscopic magnetic nature of a novel Na battery material, P2-$Na_{0.5}VO_2$, in which V ions form a two-dimensional triangular lattice, by means of muon-spin rotation and relaxation (μ^+SR) measurements down to 50 mK. Although magnetization measurements indicated the presence of an antiferromagnetic transition at 13 K, the internal magnetic field due to the formation of magnetic order appears not at 13 K but at 2 K. Furthermore, the magnetic order is found to have a wide field distribution even at 50 mK. Such wide field distribution is reasonably explained by a combination of multiple muon sites and the formation of a long-range magnetic order, while the reliable spin structure is still unknown.

1 Introduction

Based on a Hubbard model for the two-dimensional triangular lattice (2DTL), the magnetic ground state of 2DTL is predicted to change both with U/t and n, where U is the on-site Coulomb repulsion, t is the hopping integral between the nearest-neighbor sites, and n is the electron filling. In fact, for the half-filling case ($n = 1/2$), a theoretical study[1] predicts that the system is a paramagnetic metal for small U, but when $U/t \geq 3.97$, it becomes a metal with an incommensurate spiral spin density wave (SDW). As U increases further, a first-order metal-insulator transition occurs at $U/t = 5.27$, and the system enters into a commensurate, three-sublattices, 120° twist SDW state.

On the other hand, for the case with $n \neq 1/2$, another theoretical study[2] proposed a complex magnetic phase diagram as a function of U/t and n. However, there is, to our knowledge, no experimental study to confirm such diagram. Indeed, the prediction that magnetic order appears at $n = 3/4$ even when $U/t = 0$ is questionable, because half of the sites are occupied by up&down spins for such filling.

Therefore, considering geometrical frustration on 2DTL, which often leads to the formation of short-range order, a sensitive local magnetic probe is suitable for investigating the variation of magnetism with n. Muon-spin rotation and relaxation (μ^+SR) is an optimal technique for such purpose due to its unique spatial and time resolution[3]. This is our motivation for the past μ^+SR experiments on Li_xCoO_2[4], Na_xCoO_2[5], K_xCoO_2[6,7], Li_xNiO_2[8], and other related 2DTL systems[9–12]. Furthermore, in order to change n, the Li and/or Na content is adjusted mainly by an electrochemical reaction. Thus, it is very difficult to prepare enough amount of samples for e.g. neutron scattering. This is the other reason that we use μ^+SR for such purpose. Actually, we have previously used this technique to demonstrate eccentric magnetic phase diagrams for Li_xCoO_2[4] and Li_xNiO_2[8].

In addition, we want to emphasize that magnetic properties of alkali transition-metal oxides naturally depend on the distribution of elements, charges, and spins in the lattice, which also determines the electrochemical properties. Therefore, although there is no direct correlation between low-temperature magnetism and high-temperature electrochemical properties, there should be a certain interrelationship between them[13,14].

A recent discovery of novel P2- and O'3-$Na_{0.5}VO_2$[15,16], in which V ions form a two-dimensional triangular lattice (see Fig. 1), naturally expands the research area of magnetism on 2DTL to a Na-V-O system. Particularly, magnetization measurements show the presence of a pronounced AF transition at $T_N^\chi \sim 13$ K for P2-$Na_{0.5}VO_2$, while neutron diffraction measurements revealed the absence of magnetic Bragg peaks down to 1.8 K[15]. In addition, the temperature dependence of heat capacity lacks a peak at T_N^χ, but shows a very broad anomaly at ~10 K[15], leading to the question on the origin of the magnetic anomaly at T_N^χ.

[a] *Toyota Central Research & Development Laboratories, Inc., 41-1 Yokomichi, Nagakute, Aichi 480-1192 Japan. Fax: +81 561 63 6448; Tel: +81 561 71 8029; E-mail: e0589@mosk.tytlabs.co.jp*
[b] *Advanced Science Research Center, Japan Atomic Energy Agency, Tokai, Ibaraki 319-1195, Japan.*
[c] *Faculty of Physics, Babes-Bolyai University, 3400 Cluj-Napoca, Romania.*
[d] *Laboratory for Muon-Spin Spectroscopy, Paul Scherrer Institut, CH-5232 Villigen PSI, Switzerland.*
[e] *ICMCB-CNRS - 87 Av. Schweitzer- F 33608 PESSAC Cedex, France.*
[f] *Department of Materials and Nanophysics, KTH Royal Institute of Technology, Electrum 229, SE16440 Kista, Sweden.*

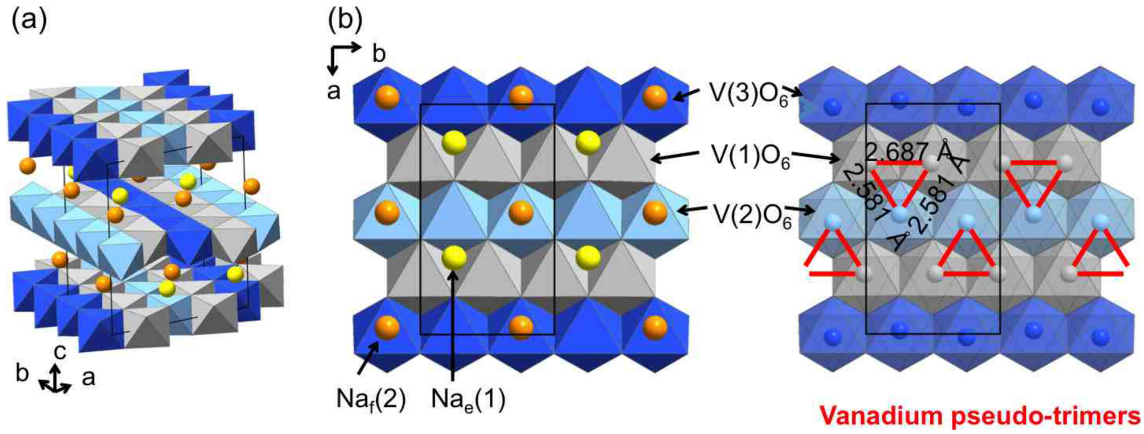

Fig. 1 (a) 3D structure of P2-$Na_{0.5}VO_2$ and (b) projection of the structure of P2-$Na_{0.5}VO_2$ along the direction perpendicular to the VO_2 planes. The unit cell is drawn with a black line.

We have, therefore, measured μ^+SR spectra mainly for P2-$Na_{0.5}VO_2$ down to 50 mK in order to elucidate the magnetic ground state. This is because μ^+SR is particularly sensitive to the local magnetic environment, because the muon mainly feels the internal magnetic field ($H_{\rm int}$) due to its nearest neighbors and is specially sensitive to the short-range magnetic order, which sometimes appears in low dimensional systems, while both neutron scattering and magnetization measurements mainly detect long-range magnetic order. In particular, if the correlation length is very short, neutron diffraction peaks broaden and eventually disappear.

2 Experiment

A powder sample of P2-$Na_{0.5}VO_2$ was synthesized in ICMCB-CNRS by sodium electrochemical deintercalation from $Na_{0.71}VO_2$ using a Na|$NaClO_4$-propylene carbonate|P2-$Na_{0.71}VO_2$ cell. The P2-$Na_{0.71}VO_2$ powder was synthesized by a solid-state reaction between $NaVO_2$ and VO_2 at 850°C for 24 h in a gold tube sealed under argon. According to powder X-ray diffraction (XRD) analysis at ambient temperature, the sample was single phase of orthorhombic symmetry with space group *Pmmn*. The structural, electrochemical, and physical properties of P2-$Na_{0.5}VO_2$ are reported elsewhere [15].

The μ^+SR spectra were recorded at a surface muon beam line using the **GPS** and **LTF** spectrometer of PSI in Switzerland. Approximately 120 mg of powder sample was pressed into a pellet with 10 mm diameter, and then placed in a titanium foil sealed copper cell for GPS or an indium wire sealed silver cell for LTF. Since the sample is very unstable in air, such work was carried out in a He-filled glove box. On GPS, the cell was attached to a low-back ground sample holder in a liquid-He flow-type cryostat for measurements in the temperature range between 1.5 and 20 K. At LTF, the silver cell was set into a dilution refrigerator (DR) down to $T = 20$ mK. Note that In enters into a superconducting state below $T_c = 3.5$ K. Thus, we did not apply external magnetic field(s) during measurements on LTF below T_c. The experimental techniques are described in more detail elsewhere [3] and the basic principle for data analyses is briefly given in Appendix 6.

3 Results

Figure 2 shows the temperature dependence of the μ^+SR spectrum obtained in a zero external magnetic field (ZF) on (a) GPS and (b) LTF. At 2 K, the ZF-spectrum exhibits a slow relaxation due to nuclear magnetic moments of ^{23}Na and ^{51}V plus ^{63}Cu and ^{65}Cu from the muons stopped in the sample cell. A rapid relaxing component is clearly seen in the early time domain below 1 μs at 1.9 and 1.5 K, indicating the appearance of an internal magnetic field ($H_{\rm int}$) due to 3*d* electrons. The spectrum at 1.5 K is almost the same as the one at 1.9 K. Even at 0.05 K, the ZF-spectrum looks very similar to 1.9 K, although the relaxation rate increases with decreasing temperature. Since we used an Ag sample holder at LTF, the background, which corresponds to the signal at $t \geq 1$ μs, is less relaxing than in the ZF-spectrum obtained with a Cu sample cell on GPS.

The overall feature of the ZF-spectrum suggests that the magnetic transition occurs not at 13 K, but at 1.9 K ($= T_{\rm m}$). Furthermore, the absence of a clear oscillation at 0.05 K is likely to indicate the lack of static long-range magnetic order, namely, the magnetic order would be random like a spin-glass state. The longitudinal field (LF) measurements at 1.5 K, which is useful to judge whether the magnetic order is random or not through the change in the relaxation with LF, revealed that random order is most unlikely (see Fig. 3). Here LF means the field parallel to the initial muon spin polarization

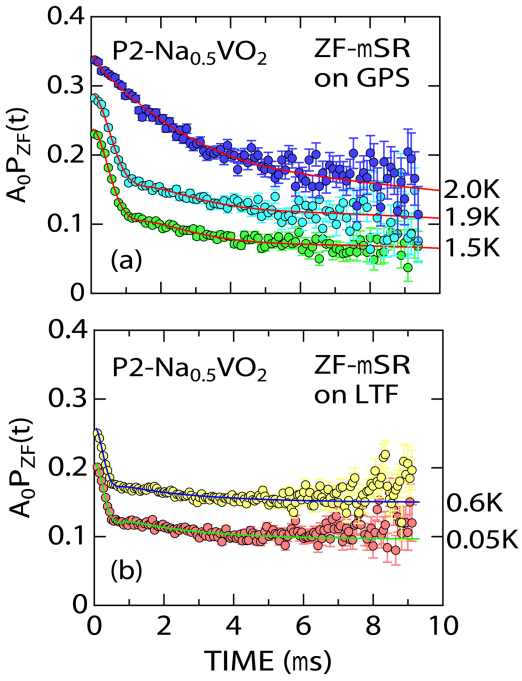

Fig. 2 ZF-μ^+SR spectrum for P2-$Na_{0.5}VO_2$ obtained (a) at 1.5, 1.9, and 2.0 K with a liquid-He flow-type cryostat on GPS and (b) at 0.05 and 0.6 K with a DR on LTF. Here, A_0 is the initial asymmetry, and for the present experiment, $A_0 = 0.25$ from the measurements of a silver reference. $P_{ZF}(t)$ is the muon spin polarization function under ZF (see text and Appendix 6). Besides the spectrum at 1.5 K in (a) and 0.05 K in (b), each spectrum is shifted upward by 0.05 for clarity of display. In (a), we used a Cu sample cell, whereas an Ag sample cell in (b).

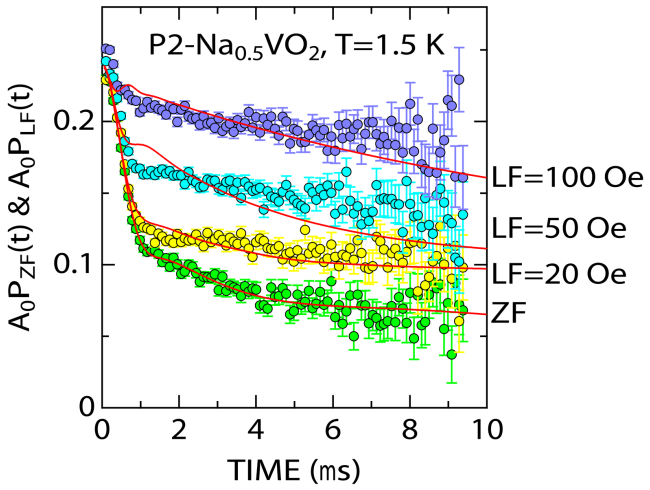

Fig. 3 ZF- and longitudinal field (LF) μ^+SR spectra for P2-$Na_{0.5}VO_2$ obtained at 1.5 K using a Cu sample cell. The applied LF was 20, 50, and 100 Oe, where LF means the filed parallel to the initial muon spin polarization. Solid lines represent the best fit using a combination of two dynamic Kubo-Toyabe functions for the Cu cell and P2-$Na_{0.5}VO_2$. The Kubo-Toyabe parameters for the Cu cell were determined by the ZF- and LF-measurements of the Cu cell alone (see text). The discrepancy between the experimental data and fitting results indicates that a Kubo-Toyabe function is not suitable for describing the internal magnetic field in P2-$Na_{0.5}VO_2$.

($\vec{S}_\mu$). Therefore, we fitted the ZF-spectrum by a combination of a Gaussian relaxing cosine oscillation for the static internal field, an exponentially relaxing non-oscillatory signal for the "1/3 tail" signal caused by fluctuations in the field component parallel to $\vec{S}_\mu$, and a background (BG) signal from the muons stopped in the Cu or Ag cell:

$$A_0 P_{ZF}(t) = A_M \exp\left(-\frac{\sigma_M^2 t^2}{2}\right)\cos(\omega_M t) + A_{tail} e^{-\lambda_{tail} t} + A_{BG} P_{BG}(t)\,, \quad (1)$$

where $f_M (\equiv \omega_M/2\pi)$ is the muon Larmor frequency corresponding to the static H_{int}, A_M, A_{tail}, and A_{BG} are the asymmetries of the three signals, and σ_M and λ_{tail} are their relaxation rates. For the Cu sample cell, P_{BG} is represented by a dynamic Kubo-Toyabe function, $G_{KT}(\Delta, \nu, t)$, where Δ is the field distribution width and ν is the field fluctuation rate. Since Δ and ν for Cu are known to show a complex temperature dependence [17], the ZF- and LF-spectra were also measured for the Cu sample cell alone. For the Ag sample cell, on the other hand, P_{BG} is given by an exponential relaxing signal, $e^{-\lambda_{BG} t}$.

The fit provided that $A_M = 0.117(2)$, $A_{tail} = 0.081(2)$, and $A_{BG} = 0.040(2)$ at 1.5 K for the data obtained on GPS with the Cu cell. Here, A_{BG} was estimated from the LF measurements of the Cu cell at 1.5 K. More correctly, at first, we determined $\Delta = 0.361(2) \times 10^6$ s^{-1} and $\nu = 0.171(9) \times 10^6$ s^{-1} for the Cu cell at 1.5 K. Then, the ZF- and LF-spectra of the sample obtained at 1.5 K were fitted with Eq. (1) using the above Δ and ν, but A_{BG} as a free parameter. Because of the rapid decay of the A_M signal, it is difficult to separate A_M and A_{tail} correctly, although A_{tail} should be equivalent to $1/2A_M$.

Figure 4 shows the temperature dependences of f_M, σ_M, and their ratio $\sigma_M/\omega_M = \sigma_M/(2\pi f_M)$. The $f_M(T)$ curve exhibits an order-parameter like temperature dependence, as expected. The magnitude of σ_M also increases with decreasing temperature, while σ_M/ω_M is found to decrease slightly with decreasing temperature. Eventually, $\sigma_M/\omega_M (\sim 1)$ is almost temperature independent, meaning that the field distribution does not change with T below T_m. In other words, the $f_M(T)$, $\sigma_M(T)$, and $\sigma_M/\omega_M(T)$ curves indicate that P2-$Na_{0.5}VO_2$ undergoes a magnetic transition at T_m, but no additional transitions down to 0.05 K. Note that the magnetic order

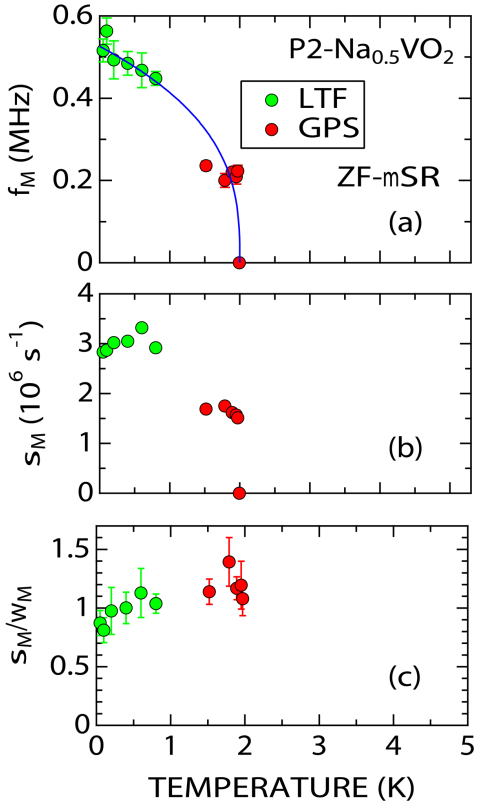

Fig. 4 The temperature dependences of (a) the muon-spin precession frequency (f_M), (b) the Gaussian relaxation rate of the precession signal (σ_M), and (c) their ratio $\sigma_M/\omega_M = \sigma_M/(2\pi f_M)$ for P2-$Na_{0.5}VO_2$. The data were obtained by fitting the ZF spectrum using Eq. (1). A solid line in (a) shows the power law fit $[f(T)/f(0\ \mathrm{K}) = [(T_m - T)/T_m]^{\gamma}]$, where $f_M(0\ \mathrm{K}) = 0.53(3)$ MHz, $T_m = 2.00(2)$ K, and a critical exponent $\gamma = 0.35(7)$.

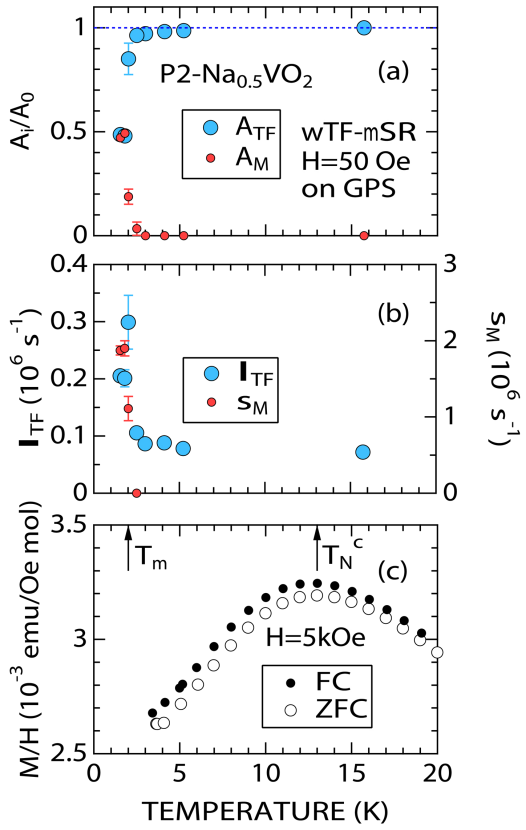

Fig. 5 The temperature dependences of (a) the two normalized asymmetries, A_{TF}/A_0 and A_M/A_0 and (b) their relaxation rates (λ_{TF} and $\sigma_{M,TF}$), and (c) susceptibility ($\chi = M/H$)[15] for P2-$Na_{0.5}VO_2$. Since $A_{TF} \sim A_0 = 0.25$ in the temperature range between 2.5 and 15 K, the whole volume of the sample is paramagnetic above 2.5 K.

in P2-$Na_{0.5}VO_2$ looks very different from a usual long-range AF order, for which $\sigma_{AF}/\omega_{AF} \ll 1$. Besides a spin-glass like freezing, such a broad field distribution is usually explained by one the following three scenarios; namely, the formation of a short-range ordered state, the appearance of a complex order[18–21], or the presence of multiple muon-sites in the lattice even for a simple long-range order. We will discuss the origin of the broad field distribution later.

In order to study the change in the volume of the paramagnetic phase, Fig. 5 shows the temperature dependences of the fitted μ^+SR parameters obtained from weak transverse field (wTF) measurements with $H_{TF} = 50$ Oe on GPS. Here, wTF means that $\vec{H}_{TF} \perp \vec{S}_\mu$ and usually $|H_{TF}| \ll |H_{int}|$. However, based on the ZF measurements, $|H_{TF}| \geq |H_{int}|$ in this case. Hence, the wTF-spectra were fitted by:

$$A_0 P_{TF}(t) = A_{TF} \exp\left(-(\lambda_{TF} t)^{\beta}\right) \cos(\omega_{TF} t + \phi_{TF}) + A_{M,TF} \exp\left(-\frac{\sigma_{M,TF}^2 t^2}{2}\right) \cos(\omega_{M,TF} t + \phi_{M,TF}) \quad (2)$$

where A_{TF} is the asymmetry for the oscillatory signal due to applied wTF and A_M is the same to that in Eq. (1). Due to the effect of wTF, $\sigma_{M,TF} \neq \sigma_M$, $\omega_{M,TF} \neq \omega_M$, and $\phi_{M,TF} \neq 0$. We also assume that the tail component, which appears below T_m, provides the oscillatory signal by wTF, i.e. A_{TF} consists not only of the contributions from the paramagnetic phase in the sample but also A_{BG} and A_{tail}. This is the reason why we use a stretched exponential relaxation for the wTF oscillatory signal. In fact, $\beta = 1$ at $T > 2.5$ K, but $\beta \sim 0.5$ at $T \leq 2.5$ K.

Since $A_{TF} = A_0 = 0.25$ at 15 K, which is the maximum value for the present setup, the whole volume of the sample is found to be paramagnetic. As temperature decreases from

15 K, such behavior is observed down to 2.5 K, then, A_{TF}/A_0 suddenly decreases and becomes a constant (~ 0.5) below 2 K. On the contrary, A_M signal appears at $T = 2.5$ K and levels off to $A_M/A_0 \sim 0.5$, with further lowering temperature. Furthermore, λ_{TF} looks independent of temperature down to just above T_m. This clearly demonstrates that the magnetic transition occurs not at 13 K but at ~ 2 K, from the viewpoint of the change in volume of each phase. The transition width (ΔT_m) is estimated as about 0.5 K, since the A_M levels off at $T \leq 2.0$ K. The present μ^+SR results are, thus, consistent with those of neutron and heat capacity measurements [15].

4 Discussion

Here, we wish to point out a few possibilities for the spin structure below T_m. Based on magnetization and resistivity measurements [15], P2-$Na_{0.5}VO_2$ is assigned as a Curie-Weiss insulator with a negative Weiss temperature ($\Theta_W = -7.4$ K). Considering the Na ordering pattern, both V^{3+} (d^2) and V^{4+} (d^1) ions are thought to coexist in the lattice. This situation is slightly different from the related compound, $Na_{0.5}CoO_2$, which is a Pauli-paramagnetic metal above $T_N \sim 88$ K [22]. Also, both ZF-μ^+SR and neutron diffraction clearly detect the formation of static AF order below T_N [23–25].

LF measurements below T_m reveal that the spin-glass freezing state is most unlikely a ground state for P2-$Na_{0.5}VO_2$ (Fig. 3). In fact, for the spin-glass freezing state, we usually expect that localized moments appear far above the freezing temperature (T_f) and then evolve with decreasing temperature towards T_f. As a result, λ_{TF} gradually increases with decreasing temperature and the $A_{TF}(T)$ curve often indicates a wide transition width. Since such behavior is not observed for P2-$Na_{0.5}VO_2$, the spin-glass freezing state is excluded as a ground state.

In the P2-$Na_{0.5}VO_2$ lattice, there are six different oxygen sites [15], implying the presence of six different muon sites about 1 Å away from each O^{2-}. Since electrostatic potential (E_p) calculations predict that $E_p = -13.5 \pm 0.7$ eV for the six sites, the implanted muons are most likely to sit at each site. Then, dipole field calculations at the six muon sites provide a wide field distribution (see Appendix 7) even for the stripe-type AF order proposed for $Na_{0.5}CoO_2$ [25] and the *A*-type AF order proposed for $Na_{0.75}CoO_2$ [26–28] and $NaNiO_2$ [29,30]. Here, in the the *A*-type AF order, the magnetic moments align ferromagnetically in the *ab* plane but antiferromagnetically along the *c*-axis.

If well-distinct multiple muon-spin precession frequencies are extracted from a ZF-μ^+SR spectrum, we could conjecture the spin structure by μ^+SR [12,31–35]. However, since there is only one f_M below T_m, it is impossible to determine the most probable AF spin structure based on the present result. Furthermore, although the wide field distribution below T_m in P2-$Na_{0.5}VO_2$ is reasonably explained using a combination of multiple muon sites and a relatively popular AF spin structure, the formation of a short-range order or a complex order is still not excluded. In order for further clarifying the spin structure, it is definitely required to perform neutron diffraction measurements well below T_m.

Back to the comparison between theory and experiment, since P2-$Na_{0.5}VO_2$ is an insulator, the distribution of *d* electron in the VO_2 plane should be inhomogeneous, i.e. both V^{3+} ($S = 1$) and V^{4+} ($S = 1/2$) coexist. Furthermore, the formation of V pseudo-trimers alters the VO_2 plane from an ideal 2DTL to isolated triangles. As a result, it is very difficult to predict the magnetic ground state of P2-$Na_{0.5}VO_2$ by a simple Hubbard model.

The fact that $T_m = 2$ K, however, indicates a relatively weak magnetic interaction between V ions compared with that in $Na_{0.5}CoO_2$. This would make Na^+ ions mobile in P2-$Na_{0.5}VO_2$ at ambient temperature [15], despite its insulating nature.

5 Acknowledgments

We thank the staff of PSI for help with the μ^+SR experiments. DA acknowledges financial support from the Romanian UEFISCDI Project PN-II-ID-PCE-2011-3-0583 (85/2011). This work was supported by MEXT KAKENHI Grant No. 23108003 and JSPS KAKENHI Grant No. 26286084.

6 Appendix; μ^+SR

When spin-polarized muons are implanted into a magnetically ordered material in ZF, the muon-spins precess around the local magnetic fields H_{int} in the material at the frequency, $\omega/2\pi = f = \gamma_\mu/2\pi \times H_{int}$, where $\gamma_\mu (= 13.554$ kHz/Oe) is the muon gyromagnetic ratio. Such oscillation in the ZF-spectrum is represented by;

$$A_0 P_{ZF}(t) = A_0\{\frac{2}{3}G_x(t)\cos(\omega t) + \frac{1}{3}G_z(t)\}. \quad (3)$$

Here, A_0 is the initial asymmetry, and for the present experiment, $A_0 = 0.25$ from the measurements of a silver reference. $P_{ZF}(t)$ is the muon spin polarization function under ZF.

Both $G_x(t)$ and $G_z(t)$ are the relaxation function caused by inhomogeneous distribution of H_{int} at the muon sites. Here, $G_z(t)$ corresponds to the relaxation of H_{int} parallel to the initial muon-spin direction (S_μ) and shows only dynamic depolarization, while $G_x(t)$ corresponds to the relaxation of $H_{int} \perp S_\mu$ and includes both static and dynamic depolarization. The $G_z(t)$ component is usually called as a "1/3" tail signal.

When there are multiple muon sites with different $H_{\rm int}$s, the ZF spectrum is given by;

$$A_0 P_{\rm ZF}(t) = \sum_{i=1}^{n} A_i \{ \frac{2}{3} G_x^i(t) \cos(\omega t) + \frac{1}{3} G_z^i(t) \}, \quad (4)$$

where n is the number of the muon sites and $\sum_{i=1}^{n} A_i = A_0$. A_i/A_0 represents the fraction of the muon sites with $H_{\rm int}^i$ to the all sites.

7 Appendix; AF spin structure

According to electrostatic potential calculations, the implanted muons are predicted to sit at the following six sites; that is, (0.4024, 0.0437, 0.1818), (0.0957, -0.0135, 0.8185), (0.1982, 0.25, 0.1684), (0.1918, 0.25, 0.3281), (0.3534, 0.25, 0.6966), and (0.3463, 0.25, 0.8203). Then, dipole field calculations provide the internal magnetic field for each muon site, if we assume a certain AF spin structure.

Figure 6 shows the calculated distribution of $H_{\rm int}$ for the stripe-type and A-type AF ordered states together with the Fourier transform amplitude ($A_{\rm Fourier}$) of the ZF-μ^+SR time-spectrum at 0.05 K. The former is proposed for $Na_{0.5}CoO_2$ by neutron[25], whereas the latter for $Na_{0.75}CoO_2$[27,28]. Both states are consistent with the present μ^+SR result, because the Fourier transformed frequency spectrum has only one broad maximum at around 0.5 MHz. In other words, we cannot determine the AF spin structure, based only on the present μ^+SR results.

If we compare the $H_{\rm int}/\mu_{\rm V}$ at which $\frac{1}{n}\sum_{i=1}^{n} D_i = 0.5$ with $H_{\rm int}$ at which $\int_0^f A_{\rm Fourier} df = 0.5 \int_0^{5{\rm MHz}} A_{\rm Fourier} df$, the ordered V moment ($\mu_{\rm V}$) is evaluated as 0.11 $\mu_{\rm B}$ [0.2 $\mu_{\rm B}$] at 0.05 K for a stripe-type state [an A-type state].

References

1 H. R. Krishnamurthy, C. Jayaprakash, S. Sarker and W. Wenzel, *Phys. Rev. Lett.*, 1990, **64**, 950–953.
2 M. Fujita, M. Ichimura and K. Nakao, *J. Phys. Soc. Jpn.*, 1991, **60**, 2831–2834.
3 G. M. Kalvius, D. R. Noakes and O. Hartmann, in *Handbook on the Physics and Chemistry of Rare Earths*, ed. K. A. Gschneidner, L. E. Jr. and G. H. Lander, North-Holland, Amsterdam, 2001, vol. 32, ch. 206.
4 K. Mukai, Y. Ikedo, H. Nozaki, J. Sugiyama, K. Nishiyama, D. Andreica, A. Amato, P. L. Russo, E. J. Ansaldo, J. H. Brewer, K. H. Chow, K. Ariyoshi and T. Ohzuku, *Phys. Rev. Lett.*, 2007, **99**, 087601.
5 J. Sugiyama, J. H. Brewer, E. J. Ansaldo, H. Itahara, T. Tani, M. Mikami, Y. Mori, T. Sasaki, S. Hébert and A. Maignan, *Phys. Rev. Lett.*, 2004, **92**, 017602.
6 J. Sugiyama, H. Nozaki, Y. Ikedo, K. Mukai, J. H. Brewer, E. J. Ansaldo, G. D. Morris, D. Andreica, A. Amato, T. Fujii and A. Asamitsu, *Phys. Rev. Lett.*, 2006, **96**, 037206.
7 J. Sugiyama, Y. Ikedo, P. L. Russo, H. Nozaki, K. Mukai, D. Andreica, A. Amato, M. Blangero and C. Delmas, *Phys. Rev. B*, 2007, **76**, 104412.
8 J. Sugiyama, H. Nozaki, Y. Ikedo, P. L. Russo, K. Mukai, D. Andreica, A. Amato, T. Takami and H. Ikuta, *Phys. Rev. B*, 2008, **77**, 092409.
9 J. Sugiyama, Y. Ikedo, K. Mukai, J. H. Brewer, E. J. Ansaldo, G. D. Morris, K. H. Chow, H. Yoshida and Z. Hiroi, *Phys. Rev. B*, 2006, **73**, 224437.
10 J. Sugiyama, H. Nozaki, Y. Ikedo, K. Mukai, P. L. Russo, D. Andreica, A. Amato, H. Yoshida and Z. Hiroi, *Phys. Rev. B*, 2008, **78**, 104427.
11 J. Sugiyama, K. Mukai, Y. Ikedo, H. Nozaki, M. Månsson and I. Watanabe, *Phys. Rev. Lett.*, 2009, **103**, 147601.
12 J. Sugiyama, K. Mukai, H. Nozaki, M. Harada, M. Månsson, K. Kamazawa, D. Andreica, A. Amato and A. D. Hillier, *Phys. Rev. B*, 2013, **87**, 024409.
13 C. M. Julien, A. Ait-Salah, A. Mauger and F. Gendron, *Ionics*, 2006, **12**, 21–32.
14 J. Sugiyama, Y. Ikedo, K. Mukai, H. Nozaki, M. Månsson, O. Ofer, M. Harada, K. Kamazawa, Y. Miyake, J. H. Brewer, E. J. Ansaldo, K. H. Chow, I. Watanabe and T. Ohzuku, *Phys. Rev. B*, 2010, **82**, 224412.
15 M. Guignard, C. Didier, J. Darriet, P. Bordet, E. Elkaïm and C. Delmas, *Nat Mater*, 2013, **12**, 74–80.
16 C. Didier, M. Guignard, J. Darriet and C. Delmas, *Inorganic Chemistry*, 2012, **51**, 11007–11016.
17 R. Kadono, J. Imazato, T. Matsuzaki, K. Nishiyama, K. Nagamine, T. Yamazaki, D. Richter and J.-M. Welter, *Phys. Rev. B*, 1989, **39**, 23–41.
18 Y. Imai, I. Solovyev and M. Imada, *Phys. Rev. Lett.*, 2005, **95**, 176405.
19 Y. Imai and M. Imada, *J. Phys. Soc. Jpn.*, 2006, **75**, 094713.
20 J. Sugiyama, H. Nozaki, I. Umegaki, W. Higemoto, E. J. Ansaldo, J. H. Brewer, H. Sakurai, T.-H. Kao, H.-D. Yang and M. Månsson, *Phys. Rev. B*, 2014, **89**, 020402.
21 J. Sugiyama, H. Nozaki, I. Umegaki, W. Higemoto, E. J. Ansaldo, J. H. Brewer, H. Sakurai, T.-H. Kao, H.-D. Yang and M. Månsson, *J. Phys.: Confer. Series*, 2014, **551**, 012011.
22 M. L. Foo, Y. Wang, S. Watauchi, H. W. Zandbergen, T. He, R. J. Cava and N. P. Ong, *Phys. Rev. Lett.*, 2004, **92**, 247001.
23 P. Mendels, D. Bono, J. Bobroff, G. Collin, D. Colson, N. Blanchard, H. Alloul, I. Mukhamedshin, F. Bert, A. Amato and A. D. Hillier, *Phys. Rev. Lett.*, 2005, **94**, 136403.
24 J. Sugiyama, Y. Ikedo, P. Russo, K. Mukai, H. Nozaki, J. Brewer, E. Ansaldo, K. Chow, D. Andreica, A. Amato, T. Fujii, A. Asamitsu, K. Ariyoshi and T. Ohzuku, *Journal of Materials Science: Materials in Electronics*, 2008, **19**, 883–893.
25 G. Gašparović, R. A. Ott, J.-H. Cho, F. C. Chou, Y. Chu, J. W. Lynn and Y. S. Lee, *Phys. Rev. Lett.*, 2006, **96**, 046403.
26 J. Sugiyama, H. Itahara, J. H. Brewer, E. J. Ansaldo, T. Motohashi, M. Karppinen and H. Yamauchi, *Phys. Rev. B*, 2003, **67**, 214420.
27 S. Bayrakci, I. Mirebeau, P. Bourges, Y. Sidis, M. Enderle, J. Mesot, D. Chen, C. Lin and B. Keimer, *Phys. Rev. Lett.*, 2005, **94**, 157205.
28 L. Helme, A. Boothroyd, R. Coldea, D. Prabhakaran, D. Tennant, A. Hiess and J. Kulda, *Phys. Rev. Lett.*, 2005, **94**, 157206.
29 C. Darie, P. Bordet, S. de Brion, M. Holzapfel, O. Isnard, A. Lecchi, J. E. Lorenzo and E. Suard, *The European Physical Journal B - Condensed Matter and Complex Systems*, 2005, **43**, 159–162.
30 M. Lewis, B. Gaulin, L. Filion, C. Kallin, A. Berlinsky, H. Dabkowska, Y. Qiu and J. Copley, *Phys. Rev. B*, 2005, **72**, 014408.
31 H. Nozaki, M. Janoschek, B. Roessli, J. Sugiyama, L. Keller, J. H. Brewer, E. J. Ansaldo, G. D. Morris, T. Takami and H. Ikuta, *Phys. Rev. B*, 2007, **76**, 014402.
32 P. L. Russo, J. Sugiyama, J. H. Brewer, E. J. Ansaldo, S. L. Stubbs, K. H. Chow, R. Jin, H. Sha and J. Zhang, *Phys. Rev. B*, 2009, **80**, 104421.
33 O. Ofer, Y. Ikedo, T. Goko, M. Månsson, J. Sugiyama, E. J. Ansaldo, J. H. Brewer, K. H. Chow and H. Sakurai, *Phys. Rev. B*, 2010, **82**, 094410.
34 J. Sugiyama, H. Nozaki, M. Månsson, K. Prša, D. Andreica, A. Amato, M. Isobe and Y. Ueda, *Phys. Rev. B*, 2012, **85**, 214407.

35 J. Sugiyama, H. Nozaki, K. Miwa, H. Yoshida, M. Isobe, K. Prša, A. Amato, D. Andreica and M. Månsson, *Phys. Rev. B*, 2013, **88**, 184417.

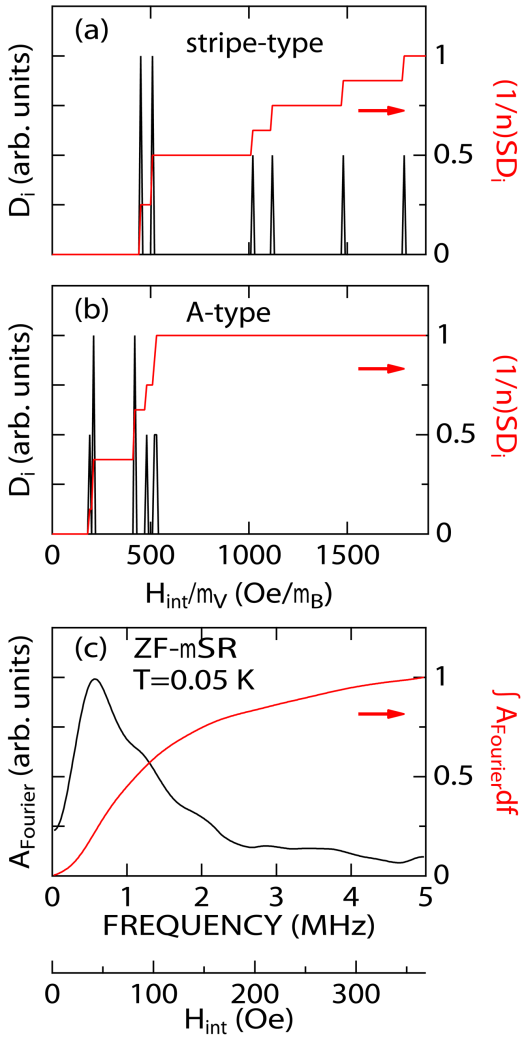

Fig. 6 Dipole field distribution for (a) the stripe-type AF order and (b) *A*-type AF order, and (c) the Fourier transformed frequency spectrum of the ZF-μ^+SR time spectrum at 0.05 K for P2-$Na_{0.5}VO_2$.